17th Brazilian Congress of Thermal Sciences and Engineering
November 25th-28th, 2018, Águas de Lindóia, SP, Brazil

ENCIT-2018-0401
SENSIBILITY STUDY OF MOMENTUM EQUATION MODELS FOR SUBCOOLED BOILING PHENOMENA SIMULATION

Brian de Lima Curtt
Francisco A. Braz Filho
Instituto de Estudos Avançados (IEAv)
Trevo Coronel Aviador José Alberto Albano do Amarante, 1, Putim
12228-001 São José dos Campos, SP
brian.curtt@gmail.com, fbraz@ieav.cta.br

Abstract. *The sensitivity of ANSYS FLUENT momentum models in the simulation of subcooled boiling flow is studied. Aiming for the prediction of nuclear industry related transients, this paper intends to establish the foundation of more specific applications in design and safety analysis of water-cooled nuclear power plants. For this, a heated channel is modeled and submitted to forced convection boiling. Momentum equation components like turbulence, boiling and interfacial transfer models are reviewed and systematically tested. Key parameters for estimation of simulation quality are chosen allowing comparison and selection of proper modeling options. A set of promising models for the future prediction of the critical heat flux is established, indicating the relevance of turbulent dispersion model in the void fraction calculation.*

Keywords: *subcooled boiling phenomena, sensibility study, momentum, CFD.*

1. INTRODUCTION

A greater comprehension of two-phase flow phenomena is of major relevance for nuclear industry applications. Even though a lot of resources have been spent studying its mechanisms and developing tools for its application in the design and safety analysis of nuclear systems, many aspects of subcooled boiling flow behavior have yet to be fully realized.

This relevance arises because water-cooled nuclear reactors are designed to operate under two-phase convection as the primary heat transfer mechanism, meaning that the bulk coolant temperature is usually kept below its saturation point. This heat transfer regime is named subcooled flow boiling and is characterized by the nucleation of bubbles at the heated surfaces, their detachment and further collapse at the subcooled region (Collier and Thome, 1994).

The study of this specific flow regime is justified due to its influences on the heat transfer coefficient, on the reactor core reactivity and on the boron deposition on the fuel cladding. Furthermore, two-phase regime can lead to abrupt changes of pressure drop flow, causing flow instabilities that can put at risk the reactor safety and compromise the power output.

For the complete evaluation of the subcooled flow boiling, two-phase modeling is essential for the prediction of the thermal-hydraulic performance of water-cooled reactor cores (Wallis, 1969). Depending on the scope and main goal of the analysis, different two-phase modeling approaches with different complexities must be applied.

The two-phase flow analysis usually accounts the relative motion between phase and, due to this reason, this modeling is expressed by two set of transport equations (mass, momentum and energy), named two-fluid model. Each set of transport equations is related to a phase and coupled to the other set of equations by interfacial interaction models. Thus, the numerical solution of a specific phase property field depends on the other phase.

The traditional design tools in the nuclear industry to predict these phenomena are generally based in material experiment data, aiming for conservative evaluations. However, aiming for more efficient systems, the application of best-estimate programs is increasingly becoming more present (IAEA, 2009).

Therefore, this paper focuses on the estimation of the subcooled boiling phenomena with the CFD program FLUENT 19.0, trying to define the proper models for this specific problem. The influence of the different models applied to the momentum conservation equations are tested through simulations, while the obtained behaviors should be analyzed and linked to foundations of each considered model.

2. METHODOLOGY

Subcooled boiling regime is obtained when the bulk temperature of the studied fluid is below its saturation point while a portion of it, in contact with a heated wall, is already saturated. The application of this regime may be found in

pressurized water nuclear plants. The experimental data related to this regime is usually obtained from water-cooled flow inside heated pipes submitted to boundary conditions in the range of nuclear power plants operation.

Experiments from Bartolomei and Chanturiya (1967) are used as references for test cases of the sensibility study. Its domain consists of a vertical circular pipe with internal diameter of 15.4 mm and heated stainless-steel walls, in which water flows upward.

From the data available, only one case is considered for this paper, being characterized by: fluid pressure of 4.5 MPa, wall heat flux of 0.57 MW.m^{-2} and inlet mass flux of 900 kg.m^{-2}.s^{-1}. Bartolomei and Chanturiya (1967) provide results of the following parameters: temperature of the inner surface of the channel wall, temperature along the flow axis, bulk flow temperature and true vapor content (void fraction). Although experiment statistics are not provided by this reference, these are the main parameters applied for the quality estimation of this paper's simulations.

Once the domain was set, its geometry and discretization in meshes were elaborated considering a two-dimensional axisymmetric flow through *DesignModeler* and *Mesh*, respectively, which are tools available in the student version platform ANSYS WORKBENCH 19.0. Available in the same platform, the software FLUENT 19.0 were applied for the flow solution, meaning the solution of the flow conservation equations.

Applying the Eulerian multiphase model available in FLUENT, the following equations for conservation of mass, conservation of momentum and conservation of energy equations, respectively, were applied (ANSYS, 2013a):

$$\frac{\partial}{\partial t}\left(\alpha_q \rho_q\right) + \nabla \cdot \left(\alpha_q \rho_q \boldsymbol{V}_q\right) = \sum_{p=1}^{n}\left(\dot{m}_{pq} - \dot{m}_{qp}\right) + S_q \tag{1}$$

$$\frac{\partial}{\partial t}\left(\alpha_q \rho_q \boldsymbol{V}_q\right) + \nabla \cdot \left(\alpha_q \rho_q \boldsymbol{V}_q \boldsymbol{V}_q\right) = -\alpha_q \nabla p + \nabla \cdot \bar{\bar{\tau}}_q + \alpha_q \rho_q \boldsymbol{g} + \sum_{p=1}^{n}\left(\boldsymbol{R}_{pq} + \dot{m}_{pq}\boldsymbol{V}_{pq} - \dot{m}_{qp}\boldsymbol{V}_{qp}\right) + \left(\boldsymbol{F}_q + \boldsymbol{F}_{lift,q} + \boldsymbol{F}_{wl,q} + \boldsymbol{F}_{vm,q} + \boldsymbol{F}_{td,q}\right) \tag{2}$$

$$\frac{\partial}{\partial t}\left(\alpha_q \rho_q h_q\right) + \nabla \cdot \left(\alpha_q \rho_q \boldsymbol{V}_q h_q\right) = \alpha_q \frac{dp_q}{dt} + \bar{\bar{\tau}} : \nabla \boldsymbol{V}_q - \nabla \cdot \boldsymbol{q}_q + S_q + \sum_{p=1}^{n}\left(Q_{pq} + \dot{m}_{pq} h_{pq} - \dot{m}_{qp} h_{qp}\right) \tag{3}$$

Where α_q is void fraction, ρ_q specific mass, $\boldsymbol{V}_q$ velocity, $\dot{m}_{pq}$ and $\dot{m}_{qp}$ interphase mass transfer, S_q the source term, p fluid pressure, $\boldsymbol{g}$ gravity acceleration, $\boldsymbol{R}_{pq}$ interphase force, $\boldsymbol{V}_{pq}$ and $\boldsymbol{V}_{qp}$ interphase velocities, $\boldsymbol{F}_q$ external body force, $\boldsymbol{F}_{lift,q}$ lift force, $\boldsymbol{F}_{wl,q}$ wall lubrication force, $\boldsymbol{F}_{vm,q}$ virtual mass force, $\boldsymbol{F}_{td,q}$ turbulent dispersion force, h_q specific enthalpy, $\boldsymbol{q}_q$ heat flux, S_q source term, Q_{pq} interphase heat exchange, h_{pq} and h_{qp} interphase enthalpy. These variables are related to p-phase or q-phase and the bold style denotes vector.

The q-phase stress-strain tensor $\bar{\bar{\tau}}_q$ is given by

$$\bar{\bar{\tau}}_q = \alpha_q \mu_q \left(\nabla \boldsymbol{V} + \nabla \boldsymbol{V}^T\right) + \alpha_q \left(\lambda_q - \frac{2}{3}\mu_q\right) \nabla \cdot \boldsymbol{V}_q \bar{\bar{I}} \tag{4}$$

While the interphase force $\boldsymbol{R}_{pq}$ is given by

$$\sum_{p=1}^{n} \boldsymbol{R}_{pq} = \sum_{p=1}^{n} K_{pq}\left(\boldsymbol{V}_p - \boldsymbol{V}_q\right) \tag{5}$$

Where μ_q and λ_q are the shear and bulk viscosity properties of q-phase, respectively, and K_{pq} is the interphase momentum exchange coefficient.

Due to the great number of models available in FLUENT 19.0 for each term in Eq. (1) to Eq. (5), an initial combination of models was obtained from Li et al. (2011) by selecting the set that showed best agreement of results with the experimental data from Bartolomei and Chanturiya (1967). Table 1 summarizes this model set which was chosen as reference for the sensibility study.

Observe that, although Li et al. (2011) used Unal correlation (Unal, 1976) for bubble departure diameter, initial tests did not obtain calculation convergence, which is the reason why this model was substituted by Tolubinski-kostanchuk (Tolubinski and Kostanchuk, 1970). About the virtual mass constant, no information was presented and FLUENT's default value was applied.

Inlet profile information was not available in either Bartolomei and Chanturiya (1967) or Li et al. (2011). To set up the domain's boundary condition, preliminary simulations considering the same channel with non-heated walls were carried out and the developed velocity, turbulence kinetic energy and specific dissipation rate profiles were applied at the channel inlet. An arbitrary temperature profile with average value of 470 K was also imposed to the channel entry.

Considering the problem as a two-phase water flow, the liquid phase properties were set to be calculated through linear interpolation considering the water states of 470.00 K and 530.60 K, both at the pressure of 4.5 MPa (Wagner and Kretzschmar, 2008). The vapor phase properties are considered constant and are obtained from its saturation state at 4.5 MPa (Wagner and Kretzschmar, 2008), simplifying this phase energy equation.

Table 1. Initial model set for sensibility study of subcooled boiling flow.

PHENOMENON	FLUENT SELECTED MODEL
Wall Boiling Model	RPI (Kurul and Podowski, 1991)
Turbulence Closure Model	k-omega SST (Menter, 1993)
Interfacial Drag Force	Ishii (Ishii, 1979)
Interfacial Lift Force	Tomiyama (Tomiyama, 1998)
Turbulent Interaction	Troshko-Hassan (Troshko and Hassan, 2001)
Turbulent Dispersion	Lopez-de-Bertodano (Lopez de Bertodano, 1991)
Interfacial Area	ia-particle (ANSYS, 2013a)
Wall Lubrication	Antal-et-al (Antal et al., 1991)
Bubble Departure Diameter	Tolubinski-kostanchuk (Tolubinski and Kostanchuk, 1970)
Nucleation Site Density	Lemmert-Chawla (Lemmert and Chawla, 1977)
Frequency of Bubble Departure	Cole (Cole, 1960)
Area of Influence Coefficient	Delvalle-kenning (Del Valle and Kenning, 1985)
Interfacial Heat Transfer Coefficient	Continuous phase-Interphase: Ranz-Marshall (Ranz and Marshall, 1952) Dispersed phase-Interphase: Lavieville-et-al (Lavieville et al., 2005)
Bubble Diameter	Unal (Unal, 1976)

Table 2. Model set variations for sensibility study of subcooled boiling flow.

CASE ID.	CHANGED MODEL	CHOSEN MODEL	CASE ID.	CHANGED MODEL	CHOSEN MODEL
Case1	-	Base case (Table 1)	*Case12*	Turbulent dispersion	Simonin (Simonin and Viollet, 1990)
Case2	Interfacial Drag Force	Universal drag (Kolev, 2005)	*Case13*	Turbulent dispersion	Burns-et-al (Burns et al., 2004)
Case3	Interfacial Drag Force	Symmetric (ANSYS, 2013a)	*Case14*	Turbulent dispersion	Diffusion-in-vof (Sokolichen et al., 2004)
Case4	Interfacial Drag Force	Schiller-Naumann (Schiller and Naumann, 1935)	*Case15*	Interfacial area	Symmetric (ANSYS, 2013a)
Case5	Interfacial Drag Force	Morsi-Alexander (Morsi and Alexander, 1972)	*Case16*	Interfacial area	Ishii (ANSYS, 2013a)
Case6	Interfacial Drag Force	Grace (Clift et al., 1978)	*Case17*	Wall lubrication	Tomiyama-et-al (Tomiyama, 1998)
Case7	Interfacial Drag Force	Tomiyama (Takamasa and Tomiyama, 1999)	*Case18*	Wall lubrication	Frank (Frank et al., 2004)
Case8	Interfacial Lift Force	Moraga (Moraga et al., 1999)	*Case19*	Wall lubrication	Hosokawa (Hosokawa et al., 2002)
Case9	Interfacial Lift Force	Saffman-Mei (Saffman, 1965)	*Case20*	Bubble departure diameter	Unal (Unal, 1976)
Case10	Interfacial Lift Force	Legendre-Magnaudet (Legendre and Magnaudet, 1998)	*Case21*	Bubble departure diameter	Kocamustafaogullari-Ishii (Kocamustafaogullari and Ishii, 1983)
Case11	Turbulent Interaction	Sato (Sato and Sekoguchi, 1979)	*Case22*	Nucleation site density	Kocamustafaogullari-Ishii (Kocamustafaogullari and Ishii, 1983)

Initial tests involved the verification of mesh dependence over results. For this, four two-dimensional meshes with different refinements were considered: grids of 12.733, 25.980, 50.918 and 50.918 (denominated 50.918b) elements. The first three meshes consist of uniform square patterns while the last one considers a bias (rectangular pattern) favoring the refinement in the region near the wall domain. The square patterns are favored since the chosen key parameters refer to cross section area averaged values or axial distributions. Despite ANSYS (2013b) declaring that wall region refinement should be avoided in combination with wall treatment models, mesh 50.918b considers it to study how it would affect the averaged parameters.

The best cost-effectiveness mesh for the next cases was chosen based on the comparison of the key parameters results with the referenced experimental data. This procedure comparison was repeated for each step described through this paper.

With these considerations, a systematic evaluation of the available components models of the momentum equation was conducted. This second group of simulations considers the change of the turbulence closure models, evaluating: *k*-ω SST (Menter, 1993), *k*-ω BSL (Menter, 1993), *k*-ω Standard (Wilcox, 1998), *k*-ε Realizable (Shih et al., 1995), *k*-ε RNG (Yakhot and Orszag, 1986), *k*-ε Standard (Launder and Spalding, 1974), Linear Pressure-Strain Reynolds stress (Gibson and Launder, 1978) and Quadratic Pressure-Strain Reynolds stress (Speziale et al., 1991). These cases are named in the results section as *Turb0* to *Turb7*, respectively.

As mentioned by ANSYS (2013b), there is no single turbulence model universally accepted as being superior for all classes of problems and the proper choice depends on the model's capabilities and limitations. Nevertheless, since the available models were not developed with subcooled boiling phenomena in mind, this tryout is a necessary procedure.

Once the proper closure model was defined, the main course (third group of simulations) of this paper was started: the variation of the different models available for each term in the momentum equation. Table 2 presents the tested configurations.

The results were treated using FLUENT 19.0 and CFX 19.0 post-processor, used to extract the defined key parameters. Besides the mentioned parameters, the void fraction radial profile was extracted in several transversal sections of the simulated domain. Since no experimental data was available for comparing these profiles, these curves were qualitatively compared looking for specific models' behaviors.

3. RESULTS

The main results of the first group of simulations, consisting of the tests for mesh refinement sensitivity, are presented in Fig. 1 to Fig. 3.

The wall temperature profile (Fig. 1) is insensible to the mesh refinement, except for the 50.918b mesh along the first half of the channel length. Due to the refinement near the wall, this mesh was expected to show some improvement when comparing with the experimental data from Bartolomei and Chanturiya (1967). However, since the experiment's inlet temperature profile is unknown, little can be said about the simulation's overall quality, only that the observed discrepancy decreases with development of the flow.

Almost the same insensibility may be observed in Fig. 2, which presents the evolution through the channel of the area averaged void fraction. A slight increase of this parameter in the region downstream the Onset of Significant Void (around 1.2 m) and by the end of the channel with the refinement increase (50.918b) are the only exceptions. Nonetheless, all options show great discrepancies with the experimental data around the distance 1.6 m from the channel inlet.

The void fraction increase induced by refinement is better observed in Fig.3, which presents the void fraction radial profile at the axial position 1.7 m (relative to the channel's inlet). It can be noticed that the profile gradient near the wall is steeper with increasing refinement, indicating a better representation of nucleation and accumulation of bubbles in this region.

The other key parameters, axial and bulk temperature profiles, are not presented since no significant changes were seen.

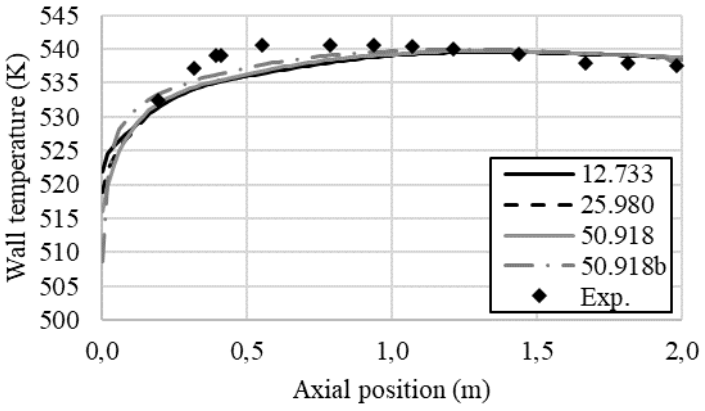

Figure 1. Wall temperature sensibility to mesh refinement.

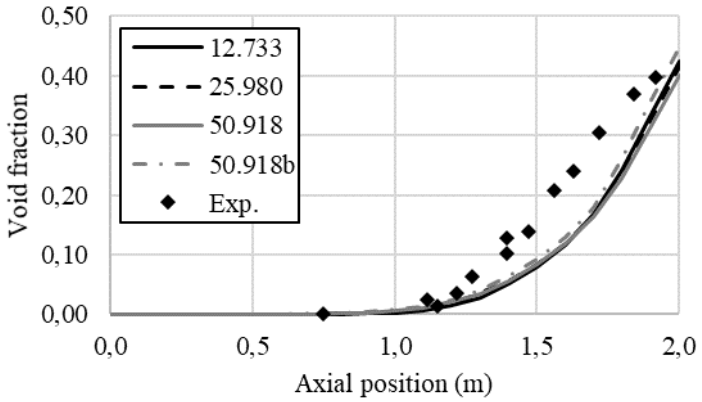

Figure 2. Void fraction sensibility to mesh refinement.

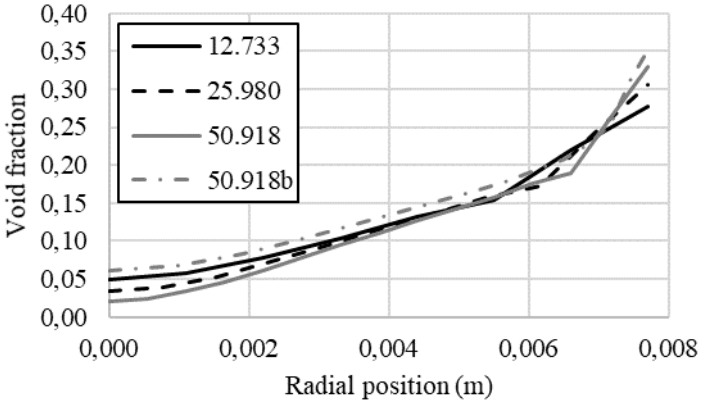

Figure 3. Void fraction radial profile at axial position 1.7 m
sensibility to mesh refinement.

Figure 4 to Fig. 7 summarize the results for the tested turbulence closure models.

Figure 4 shows great discrepancies in the wall temperature results at the first quarter of the channel, but with all calculations converging after this region. Results may be separated in two groups according to their behaviors: the *k*-ω models (*Turb0* to *Turb2*) and the other options (*Turb3* to *Turb7*). This behavior is explained by the inlet boundary conditions that were calculated using a *k*-ω model during the preliminary simulation since this data was not available in the experiments reference. Other cases were initialized with default values and, with the flow development, this source of discrepancies disappears. These results highlight the relevance of proper initial conditions for the reproducibility of experiments.

The averaged area void fraction curves in Fig. 5 show insensibility to the turbulence model at the first half of the channel length and at its end. Around 1.6 m, discrepancies of about 0.5 are seen among the simulation results. The *k*-ε Realizable (*Turb3*) shows the best agreement to this parameter's experimental data, mostly before 1.5 m. After this length, all models' results begin to converge.

The behavior at the first quarter of the channel for the axial temperature may also be explained by inlet boundary condition mentioned for the wall temperature results. After the distance of 1.5 m, the simulation temperatures split again between *k*-ω models and other options, but not due to boundary conditions issues in this case since Li et al. (2011) presented the same behavior for the *k*-ε models. Li et al. (2011) propose that the discrepancies may be explained by the wall treatment methods applied for each turbulence model, since *k*-ω models are the only models with intrinsic wall treatments.

Figure 7 shows that the radial void fraction profile is more sensitive to the turbulence model choice, influencing the curves average values and formats. The *k*-ω models show no inflection points while other models present two inflections. The curves' concavities occur in different orders for *k*-ε (*Turb3* to *Turb5*) and Reynolds stress models (*Turb6* and *Turb7*).

From the presented results, Menter's (1993) *k*-ω SST model is chosen as the best choice for the studied scenario. This model was initially developed for aerodynamics (involving external shear flow), incorporating *k*-ε formulation for

free shear layers and its transition to standard *k*-ω. Although both families of models depend on empirical constants, their formulations have enough generality.

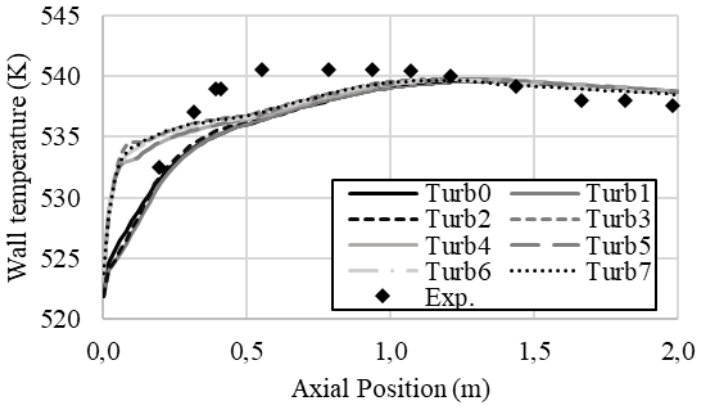

Figure 4. Wall temperature sensibility to turbulence closure models.

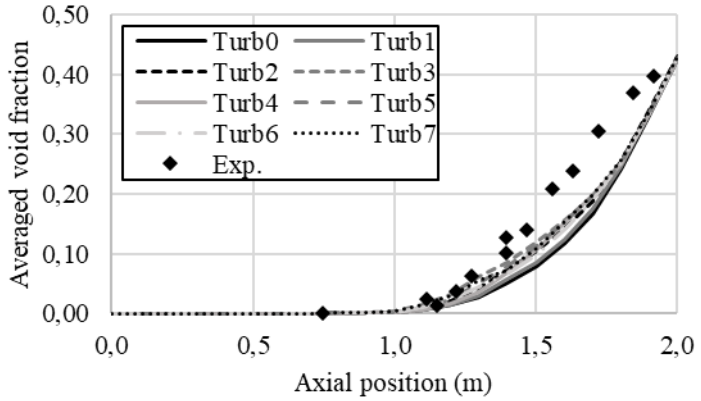

Figure 5. Void fraction sensibility to turbulence closure models.

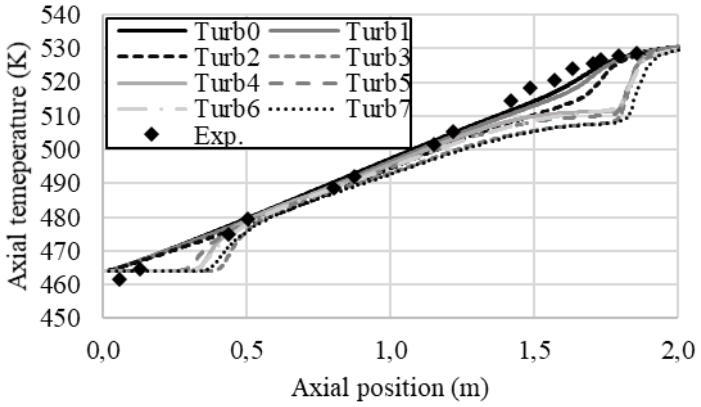

Figure 6. Temperature along the channel axis sensibility to turbulence closure models.

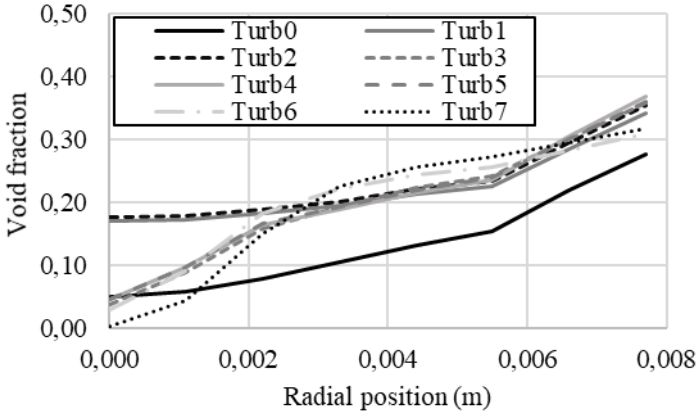

Figure 7. Void fraction radial profile at axial position 1.7 m
sensibility to turbulence closure models.

The results of the tests for momentum component models are presented in Fig. 8 to Fig.12. Since a total of 22 cases were simulated in this group, a selection of the most interesting results is presented. It must be commented that not all cases converged: most simulations had continuity residuals stuck around 10^{-4}, while *Case20* and *Case22* did not converge at all.

Case20's non-convergence is unexpected since the flow conditions are inside the correlation range of Unal's (1976) model for bubble departure diameter. It is deduced that the combination of the chosen models leads to numerical errors during FLUENT's calculation, but studies beyond the focus of this paper are necessary to confirm. The same is considered for the unexpected numerical errors occurring for *Case22*, in which Kocamustafaogullari and Ishii (1983) pool boiling based formulation is applied for the nucleation site density estimative.

Wall temperature showed to be insensitive to most of the models mentioned in Table 2, presenting behaviors like the one calculated for *Case1* (Base case) in Fig. 8. The exceptions are presented in the same figure. *Case18* presents the smallest discrepancies with experimental data in the last quarter of the channel, while keeping it analogous to *Case1* before 1.5 m. Since *Case18* applies the wall lubrication model from Frank et al. (2004), it shows that this model slightly overpredicts Antal et al.'s model (1991), in which it is based, driving the vapor away from domain's wall and leading to the obtained temperature behavior.

Case15 and *Case16* present a slight elevation of wall temperature in the last quarter of the channel's length. These cases apply Symmetric and Ishii models, respectively, being both modifications of the Particle model (ANSYS, 2013a) that ensure consistence in interfacial area estimation. Based on these formulations, it is deduced that other components of the momentum equation are not accurate enough for the prediction flow's void fraction or bubble diameters near walls when considering the areas consistence restrictions.

The wall temperature rises continuously in *Case21*, which considers Kocamustafaogullari and Ishii's (1983) correlation for bubble departure diameter based on pool boiling data. This temperature and the estimated void fraction (Fig. 9) indicate that FLUENT calculates a more inefficient heat transfer regime than when applying Lemmert and Chawla's (1977) model.

Figure 9 presents a great variation of the area averaged void fraction in the second half of the channel depending on the models applied. Most results present curves around the one obtained from *Case1*, like *Case10* and *Case14*. On the other hand, *Case13* provided a very different profile that has a very good agreement with Bartolomei and Chanturiya's (1967) data.

Case13 applies Burns et al.'s (2004) model for turbulent dispersion, which promotes the transport of discrete phase by continuous phase. Its development considered the application in Eulerian multi-phase flows with a double averaging procedure, being Lopez de Bertodano's (1991) model a particular case of this formulation. Burns et al. (2004) validate their model with bubbly flows in a vertical pipe data, indicating the applicability to this paper's case.

Legendre and Magnaudet's (1998) interfacial lift force model (*Case10*) leads to a similar void fraction curve from *Case13*, yet still strongly underestimating experimental data. The estimated force is enough to promote transport of discrete phase, but with an alternative mechanism.

Although *Case13* shows good agreement with the void fraction, Fig. 10 indicates that this model behaves similarly to the *k*-ε models around 1.6 m for the central line temperature. Meanwhile, Sokolichen et al.'s (2004) turbulent dispersion model in *Case14* presents the best agreement with experimental data in the same region of the channel. The dispersion promoted a void fraction distribution that favors this parameter estimative over area averaged void fraction (Fig. 9).

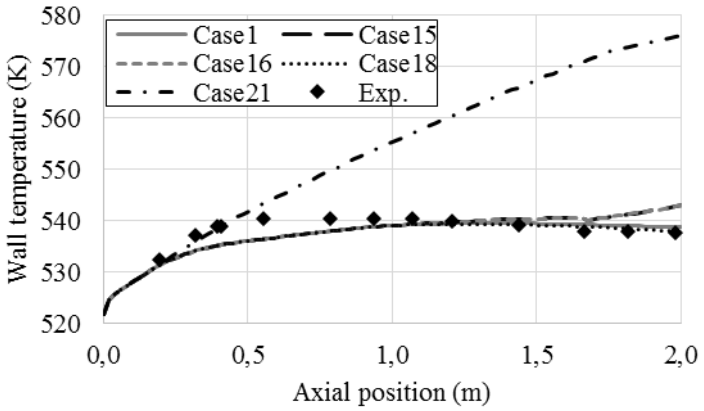

Figure 8. Wall temperature sensibility to momentum component models.

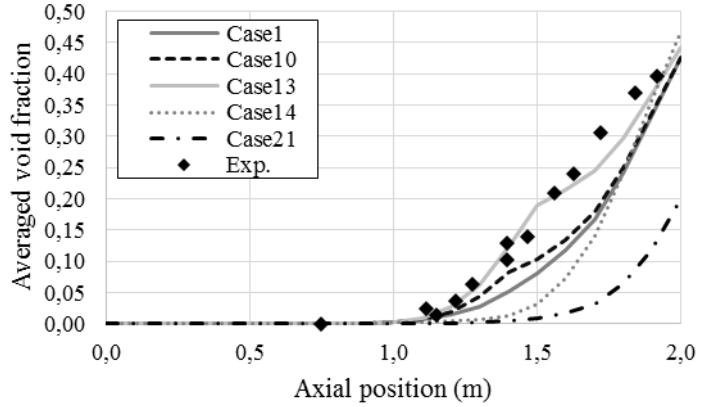

Figure 9. Void fraction sensibility to momentum component models.

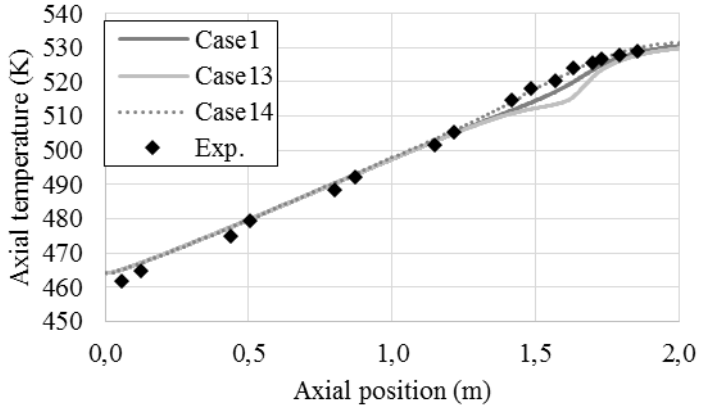

Figure 10. Temperature along the channel axis sensibility to momentum component models.

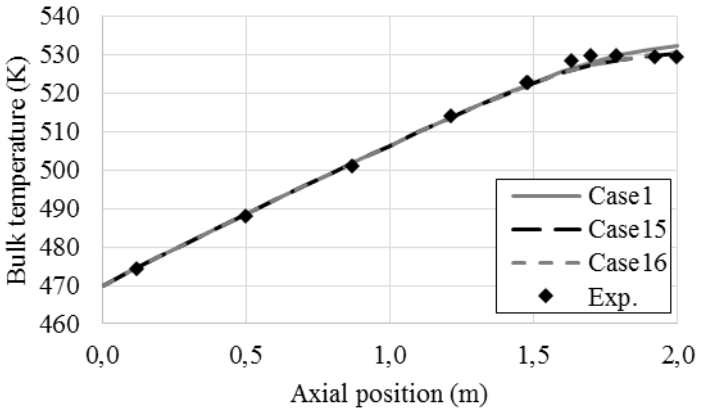

Figure 11. Bulk temperature sensibility to momentum component models.

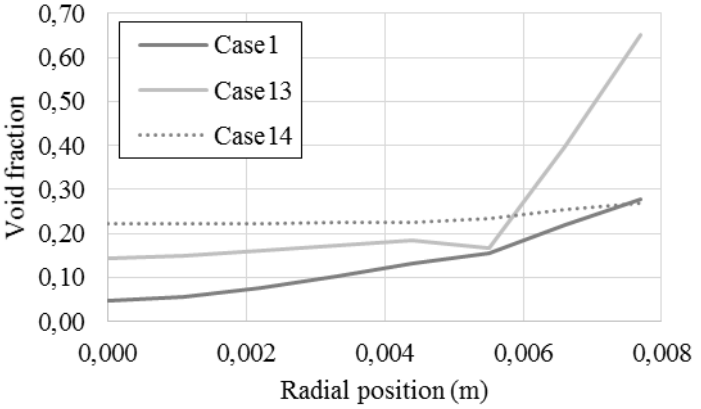

Figure 12. Void fraction radial profile at axial position 1.7 m
sensibility to momentum component models.

About the other turbulent dispersion options, Simonin and Viollet's (1990) model applied in *Case12* did not present significant discrepancies to the Base case, which applied Lopez de Bertodano's (1991) formulation.

Figure 11 presents the bulk temperature evolution along the channel. This parameter is practically identical in all the cases simulated, since it depends on the enthalpy gain along the channel. It should be observed that all simulations executed showed difficulty to approach the constant temperature region of the last quarter of the domain. *Case15* and *Case16*, which presented inefficient heat transfer by the end of the flow's domain (Fig. 8), obtained smaller temperature rise in this region.

At last, the radial void fraction profile is presented in Fig. 12, which shows that *Case13* has a greater concentration of bubbles near the wall than other models estimate. Case1's curve exemplifies the general behavior of other options and, when comparing with the results from *Case13* and *Case14,* demonstrates the turbulent dispersion effect on this distribution.

4. CONCLUSIONS

This paper summarizes a large amount of numerical experiment data obtained with the goal of looking for the key components of the momentum equation modeling necessary for a good estimation of the subcooled boiling phenomena. Results show that some model configurations may be appropriate only for specific flow parameters, demanding that the objectives of the planned analysis (depending on its application) are well defined before choosing the proper model set.

The area averaged void fraction was most influenced by changes in the turbulent dispersion models. *Case13* (Burns et al., 2004) presented the best agreement with this parameter's experimental data, while *Case14* (Sokolichen et al., 2004) had one of the worst results. Indeed, most models had difficulties to obtain the almost linear behavior of the experimental data.

Chosen models for interfacial lift force showed a lesser influence over the area averaged void fraction. In this models' group, *Case10* (Legendre and Magnaudet, 1998) led to a good agreement with experimental data with a behavior similar to *Case14*.

The correlation for bubble departure diameter in *Case21* (Kocamustafaogullari and Ishii, 1983) led to the worst void fraction prediction. At the same time, this case's wall temperature monotonically raised through the channel's length. This indicates an unexpected poor heat transfer for the studied scenario.

Central line temperature was specially influenced by the turbulence models, predicting distributions with great discrepancies with experimental data when void fraction reached values around 0.10. These models also have influence in void fraction distribution that may be related to central line temperature behavior. In these aspects, k-ω models presented consistent estimations with the expected system behavior.

These observations point out relevant models and their options in the momentum equation for prediction of the critical heat flux phenomena. The void fraction distribution, and its formation, represents a great concern to this objective that needs, therefore, further investigation.

5. REFERENCES

ANSYS, 2013a. *ANSYS Fluent Theory Guide*. ANSYS, Inc., Southpointe, Release 15.0.

ANSYS, 2013b. *ANSYS Fluent User's Guide*. ANSYS, Inc., Southpointe, Release 15.0.

Antal, S. P., Lahey, R. T. and Flaherty, J.E., 1991. "Analysis of phase distribution in fully developed laminar bubbly two-phase flow". *International Journal of Multiphase Flow*, Vol. 17, n. 5, p. 635–652.

Burns, A. D. B., Frank, T., Hamill, I. and Shi, J.-M., 2004. "The Favre Averaged Drag Model for Turbulent Dispersion in Eulerian Multi-Phase Flows". In *Fifth International Conference on Multiphase Flow – ICMF-2004*, Yokohama, Japan.

Clift, R., Grace, J. R., and Weber, M. E., 1978. *Bubbles, Drops, and Particles*. Academic Press, New York, 1978 edition.

Cole, R., 1960. "A Photographic Study of Pool Boiling in the Region of the Critical Heat Flux". *AIChE journal*, Vol. 6, p. 533–542.

Collier, J. G. and Thome, J. R.,1994. *Convective boiling and condensation*. Clarendon Press, Oxford, 3rd edition.

Del Valle, V. H. and Kenning, D. B. R., 1985. "Subcooled flow boiling at high heat flux". *International Journal of Heat and Mass Transfer*, Vol. 28, n. 10, p. 1907–1920.

Frank, T., Shi, J. M. and Burns, A. D., 2004. "Validation of Eulerian Multiphase Flow Models for Nuclear Safety Applications". In *Third International Symposium on Two-Phase Flow Modeling and Experimentation*, Pisa, Italy.

Gibson, M. M. and Launder, B. E., 1978. "Ground Effects on Pressure Fluctuations in the Atmospheric Boundary Layer". *J. Fluid Mech*. Vol. 86, p. 491–511.

Hosokawa, S., Tomiyama, A., Misaki, S., and Hamada, T., 2002. "Lateral Migration of Single Bubbles Due to the Presence of Wall". In *ASME 2002 Joint U.S.-European Fluids Engineering Division Conference*, Montreal, Canada.

IAEA, 2009. *Deterministic Safety Analysis For Nuclear Power Plants*. International Atomic Energy Agency, Vienna.

Ishii, M., 1979. "Two-fluid model for two-phase flow". In *2nd International Workshop on Two-phase Flow Fundamentals*. Troy, USA.

Kocamustafaogullari, G. and Ishii, M., 1983. "Interfacial area and nucleation site density in boiling systems". *International Journal of Heat and Mass Transfer*, Vol. 26, n. 9, p. 1377–1387.

Kolev, N. I., 2005. *Multiphase Flow Dynamics 2: Thermal and Mechanical Interactions*. Springer, Berlin, 2nd edition.

Kurul, N. and Podowski, M.Z., 1991. "On the modeling of multidimensional effects in boiling channels". In *Proceedings of the 27th National Heat Transfer Conference*. Minneapolis, USA.

Launder, B. E. and Spalding, D. B., 1974. "The numerical computation of turbulent flows". *Computer Methods in Applied Mechanics and Engineering*, Vol. 3, n. 2, p. 269-289.

Lavieville, J., Quemerais, E. , Mimouni, S., Boucker, M. and Mechitoua, N., 2005. "NEPTUNE CFD V1.0 Theory Manual", EDF.

Legendre, D. and Magnaudet, J., 1998. "The Lift Force on a Spherical Bubble in a Viscous Linear Shear Flow". *J. Fluid Mech*, Vol. 368, p. 81–126.

Lemmert, M. and Chawla, L. M., 1977. "Influence of flow velocity on surface boiling heat transfer coefficient". *Heat Transfer in Boiling*, Vol. 237, p. 247.

Li, H., Vasquez, S. A., Punekar, H. and Muralikrishnan, R., 2011. "Prediction of Boiling and Critical Heat Flux Using an Eulerian Multiphase Boiling Model", In *Proceedings of the ASME 2011 International Mechanical Engineering Congress & Exposition - IMECE2011*. Denver, USA.

Lopez de Bertodano, M., 1991. *Turbulent Bubbly Flow in a Triangular Duct*. Ph.D. thesis, Rensselaer Polytechnic Institute, Troy.

Menter, F. R.,1993. "Zonal Two Equation k-ω Turbulence Models for Aerodynamic Flows". In *23rd fluid dynamics, plasmadynamics, and lasers conference*. Orlando, USA.

Moraga, F. J., Bonetto, R. T. and Lahey, R. T., 1999. "Lateral forces on spheres in turbulent uniform shear flow". *International Journal of Multiphase Flow*, Vol. 25, p. 1321–1372.

Morsi, S. A. and Alexander, A. J, 1972. "An Investigation of Particle Trajectories in Two-Phase Flow Systems". *J. Fluid Mech*. Vol. 55, n. 2, p. 193–208.

Ranz, W. E. and Marshall, W. R. Jr., 1952. "Vaporation from Drops, Part I". *Chem. Eng. Prog*, Vol. 48, n. 3, p. 141–146.

Saffman, P. G., 1965. "The Lift on a Small Sphere in a Slow Shear Flow". *J.Fluid Mech*, Vol. 22, p. 385–400.

Sato, Y. and Sekoguchi, K., 1972. "Liquid Velocity Distribution in Two-Phase Bubbly Flow". *Int. J. Multiphase Flow*, Vol. 2, p. 79.

Schiller, L. and Naumann Z., 1935. "A drag coefficient correlation". *Z. Ver. Deutsch. Ing*, Vol. 77, p. 318-323.

Shih, T.-H., Liou, W.W., Shabbir, A., Yang, Z. and Zhu, J., 1995. "A New k-ε Eddy-Viscosity Model for High Reynolds Number Turbulent Flows - Model Development and Validation". *Computers Fluids*, Vol. 24, n. 3, p. 227–238.

Simonin, O. and Viollet, P. L., 1990. "Modeling of Turbulent Two-Phase Jets Loaded with Discrete Particles". *Phenomena in Multiphase Flows*. Vol. 1, p. 259–269.

Sokolichen, A., Eigenberger, G. and Lapin, A, 2004. "Simulation of Buoyancy Driver Bubbly Flow: Established Simplifications and Open Questions". *AIChE Journal*, Vol. 50, n. 1. P. 24–45.

Speziale, C. G., Sarkar, S. and Gatski, T. B., 1991. "Modelling the Pressure-Strain Correlation of Turbulence: An Invariant Dynamical Systems Approach". *J. Fluid Mech*, Vol. 227, p. 245–272.

Takamasa, T. and Tomiyama, A., 1999. "Three-Dimensional Gas-Liquid Two-Phase Bubbly Flow in a C-Shaped Tube". In *Ninth International Topical Meeting on Nuclear Reactor Thermal Hydraulics (NURETH-9)*. San Francisco, USA.

Tolubinski, V. I. and Kostanchuk, D. M., 1970. "Vapor bubbles growth rate and heat transfer intensity at subcooled water boiling". In *4th International Heat Transfer Conference*, Paris, France.

Tomiyama, A., 1998. "Struggle with computational bubble dynamics". In *Third International Conference on Multiphase Flow*. Lyon, France.

Troshko, A. A. and Hassan, Y. A., 2001. "A Two-Equation Turbulence Model of Turbulent Bubbly Flow". *International Journal of Multiphase Flow*, Vol. 27, n. 11, p. 1965-2000.

Unal, H. C., 1976. "Maximum Bubble Diameter, Maximum Bubble Growth Time and Bubble Growth Rate During Subcooled Nucleate Flow Boiling of Water Up To 17.7 MN/m²". *Int. J. Heat Mass Transfer*, Vol. 19, p. 643–649.

Wagner, W. and Kretzschmar, H., 2008. "IAPWS industrial formulation 1997 for the thermodynamic properties of water and steam". *International Steam Tables: Properties of Water and Steam Based on the Industrial Formulation IAPWS-IF97*, p. 7-150.

Wallis, G. B., 1969. *One Dimensional Two-Phase Flow*. McGraw-Hill, New York, 1st edition.

Wilcox, D. C., 1998. *Turbulence Modeling for CFD*. DCW Industries, Inc, La Canada.

Yakhot, V. and Orszag, S. A., 1986. "Renormalization Group Analysis of Turbulence I Basic Theory". *Journal of Scientific Computing*, Vol. 1, n. 1, p. 1–51.

6. RESPONSIBILITY NOTICE

The authors are the only responsible for the printed material included in this paper.